Gümüşhane University Journal of Science

GUFBD / *GUJS* (2023) 13(1): 199-209 doi: 10.17714/gumusfenbil.1092658 Research Article

Assessment of harmonic mitigation performance of electric springs with different inverter topologies

Farklı inverter topolojili elektrikli yayların harmonik azaltma performanslarının değerlendirilmesi

Turgay DUMAN*[1], Kadir DOĞANŞAHİN [2]

[1]*Erzurum Technical University, Department of Electrical and Electronics Engineering, Erzurum, TURKEY*

[2]*Artvin Çoruh University, Department of Electrical and Electronics Engineering, Artvin, TURKEY*

• Received: 24.03.2022 • Accepted: 08.12.2022

Abstract

Electric spring (ES) is a new technology inspired by the idea of realization a system that is equivalent to mechanical springs in terms of functionality within power systems. Electric springs are comprised from a DC voltage source, an inverter and an LC filter at the grid side. It can be used effectively in power systems to perform many functions such as voltage regulation, reactive power compensation, demand management and energy storage. On the other hand, due to the semiconductor elements in ES structure, it causes distortion on voltage and current waveforms. However, various control approaches have been proposed in the literature in order to prevent the aforementioned distortions. In this study, three different ESs has been modeled with the inverter topologies chosen from the frequently preferred once used in applications, namely Half-Bridge, Full-Bridge, and Neutral Point Clamped Multi-Level Inverter (NPC-MLI). The disruptive effects of electric springs with different inverter topologies on the grid and their performance in harmonic elimination have been examined through the results obtained from simulations realized in MATLAB/Simulink®.

Keywords: Electric spring, Harmonics, Inverter topologies.

Öz

Elektrikli yay (ES), güç sistemlerinde işlevsellik açısından mekanik yaylara eşdeğer bir sistem gerçekleştirme fikrinden esinlenilerek geliştirilmiş yeni bir teknolojidir. Elektrikli yaylar bir DC gerilim kaynağından, bir inverterden ve şebeke tarafında bir LC filtreden oluşur. Güç sistemlerinde voltaj regülasyonu, reaktif güç kompanzasyonu, talep yönetimi ve enerji depolama gibi birçok işlevi yerine getirmek için etkin bir şekilde kullanılabilir. Öte yandan ES yapısındaki yarı iletken elemanlar nedeniyle gerilim ve akım dalga şekillerinde bozulmalara neden olur. Ancak söz konusu bozulmaların önüne geçebilmek için literatürde çeşitli kontrol yaklaşımları önerilmiştir. Bu çalışmada, uygulamalarda sıklıkla tercih edilen evirici topolojileri ile Yarım-Köprü, Tam- Köprü ve Nötr Nokta Kenetlemeli Çok-Seviyeli İnverter (NPC-MLI) olmak üzere üç farklı ES modellenmiştir. MATLAB/Simulink® programında gerçekleştirilen simülasyonlardan elde edilen sonuçlarla, farklı evirici topolojilerine sahip elektrik yaylarının şebeke üzerindeki bozucu etkileri ve harmonik gidermedeki performansları incelenmiştir.

***Anahtar Kelimeler**: Elektrikli yaylar, Harmonikler, İnverter topolojileri*

* **Turgay DUMAN**; turgay.duman@erzurum.edu.tr

1. Introduction

With the increase energy demand and rise of economic and environmental concerns, penetration of renewable energy sources in electrical power systems has enhanced. In addition, on the consumption side, there is a demanding trend in the use of smart systems that allow more efficient use of energy and interact with consumer and various systems. While the intermittent power generation of renewable energy sources cause instability on the generation side, consumption profiles change with the widespread usage of smart systems (Palensky & Dietrich, 2011). Moreover, semiconductor elements within the structure of smart systems cause distortions on voltage and current. All these aforementioned reasons reveal power quality problems in distribution systems where renewable based DG (distributed generation) and smart systems used mostly.

Voltage stability is one of the main power quality concerns experienced in distribution systems. Intermittent nature of renewable energy sources and variable load profiles make difficult to achieve supply-demand balance. Voltage sags and swells are occurred as the result of these unbalances. Systems such as OLTC (On-Load Tap Changer), STATCOM (Static Synchronous Compensator), SVR (Step Voltage Regulator) are widely used in the distribution network to provide voltage regulation (Daratha et al., 2014; Muttaqi et al., 2015; Rao et al., 2000). These voltage regulators operate based on the principle of keeping the output voltage value within the desired range specified by the standards. As one of the state of the art voltage regulation systems, electrical spring (ES) provides voltage regulation support to the system by controlling the input voltage instead of the output voltage, unlike the conventional voltage regulation systems (Shuo et al., 2014). The concept of the electric spring as a new smart grid technology was firstly introduced by Hui et al. (2012). Different topologies for ES have been proposed in the literature. Hardware structures of single-phase and three-phase ESs are presented by Q. Wang, Deng, et al. (2018). Besides voltage regulation, ES has been used for different functions such as frequency control (Q. Wang, Cheng, et al., 2018), three phase balancing (Yan et al., 2015), storage reduction in AC microgrids (M.-H. Wang et al., 2019), demand side management and power quality improvement (Lee et al., 2021) with the addition of energy storage. Different control strategies have been developed to perform these functions. Different control methods and schemes of ES have been reported (Kaymanesh et al., 2021; Liang et al., 2020; Q. Wang, Cheng, et al., 2018; Yang et al., 2018). A detailed review of the DC and AC electric springs has been reported by summarizing the operating principle, circuit topology, application and control methods (M. Wang et al., 2021).

Half bridge and full bridge converter topologies are the most common converters used in ES structure. Besides, there are also studies using multilevel converters such as cascaded H-bridge and NPC topologies as ES converters (Duman, 2021; Pawar et al., 2017; Sundar et al., 2017). The type of converter used in ES may differ in terms of distorting effects on voltage and current waveforms. Gajbhiye et al. (2018) compared the disturbing effects of half bridge, full bridge and NPC type converter topologies on voltage. Electric springs can also be operated to achieve eliminating harmonics in the input voltage while providing voltage regulation (Yan et al., 2017). A control strategy for the elimination of harmonics on input voltage of ES has been proposed by Kanjiya & Khadkikar (2013).

In this study, the distorting effects of half bridge, full bridge and NPC converters used in ES applications on voltage and current waveforms have been investigated. In addition, the control of the ES has been rearranged to eliminate voltage harmonics, beside the voltage regulation function. This control strategy has been applied to three different types of ES converter, namely half bridge, full bridge and NPC-MLI. Since these converters have different numbers of switching elements and different number of levels at the output waveforms, their distorting effects on current and voltage will be different. In order to emphasize these differences, the distortion effects of each converter on voltage and current waveforms and their performances in harmonic elimination have been presented by illustrating the results obtained from MATLAB/Simulink®.

The dynamic switching in the operation of ES during the voltage regulation activity in the power system may cause distortion on the current and voltage waveforms (Shademan et al., 2021). Considering the effect of a single ES on the power system, its distorting effect on the voltage waveform may be quite limited on grid side. However, considering the number of consumers in the distribution network, the cumulative effect of ES is significant and needs to be considered (Zheng et al., 2020). Besides, the effect of current harmonics is important for loads connected to point of common coupling (PCC) with ES. The results presented in this study may guide the decisions on the converter topology to be used in ES applications.

The remaining parts of the study is formed as follows; the next section is on the basic structure, operation principle and control of electric springs. In the third part, the results obtained from the simulation studies on the ESs formed with half bridge, full bridge and MLI NPC are discussed. In the last part, the remarkable findings are mentioned by summarizing this study.

2. Basics of electric spring

ES is an emerging technology that is connected in parallel to the systems with a serial load to regulate the voltage on the loads connected to PCC. This structure, which is formed by ES and serial load, is known as smart load in the literature. The main feature that distinguishes ES from conventional voltage regulators such as STATCOM, SVR, OLTC is to provide regulation of the input voltage at the point where it is connected and to operate with a serial load (Chaudhuri et al., 2014). Therefore, ES is a promising technology that offers local and decentralized voltage regulation. In this section, the basic structure, working principle and control strategy of ES are given in subheadings.

2.1. Electric spring structure

General application of ES in the power system is shown in Figure 1. In the system model, the grid has been modeled by a voltage source and an impedance. The voltage source represents the main bus connection point which is strong as enough to have constant voltage. Z_{line} is the impedance of the line from the connection point of the smart load to the main bus. The ES basically comprised from a DC input source, a power converter, and an LC output filter. The output current is tuned by controlling the inverter. Thus, the capacitor on the branch takes place in the system as a current-controlled voltage source. The structure formed by ES and a serial load which has low voltage sensitivity and is named as non-critical load, is connected in parallel to the power system. The load that is connected in parallel to the system from PCC is called critical load, and sensitive to voltage changes. Different configurations of ES (ES-1, ES-2, ES-3, ES-4, and DCES) have been mentioned in the literature (Tapia-Tinoco et al., 2020). This study is based on ES configuration with battery on the DC side which is known as ES-2.

2.2. Operation principle of electric spring

ES is a power electronics interface that modifies a voltage profile on the capacitor with the purpose of regulating the non-critical load voltage to be compatible with the voltage fluctuations in the system. Therefore, ES and non-critical load provide voltage regulation in a cooperative manner and this formation is called as smart load.

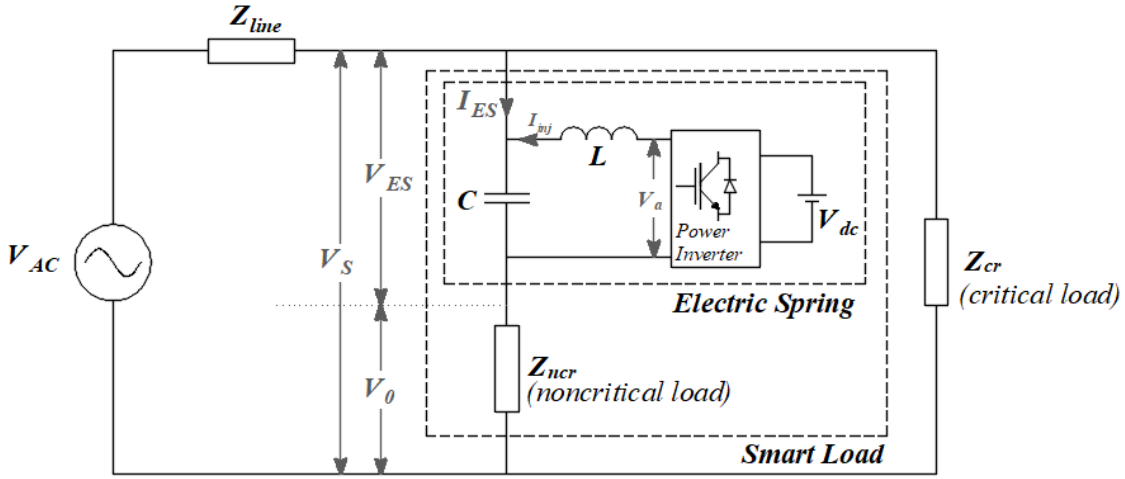

Figure 1. Schematic of a basic electric power system with an electric spring

The relationship between the voltage at PCC (V_s), the voltage of capacitor on the branch (V_{ES}), and the voltage non-critical load voltage (V_o) is given by (1).

$$V_s = V_0 + V_{ES} \quad (1)$$

$$I_{cap} = I_{ES} + I_{inj} \quad (2)$$

The current flows through the capacitor (I_{cap}) in the structure forming the smart load is equal to the sum of the phasors of the smart load current (I_{ES}) and the current injected (I_{inj}) into the system by the ES as given in (2). The phasor of the voltage on the capacitor (V_{ES}) should be perpendicular to the non-critical load current phasor (I_{ES}) to provide reactive power compensation for the purpose of voltage regulation. ES boosts PCC voltage by operating in capacitive mode in which V_{ES} leads I_{ES} by 90º (Figure 2b). On the other hand, for reducing voltage, ES operates in inductive mode in which V_{ES} lags I_{ES} by 90º (Figure 2c).

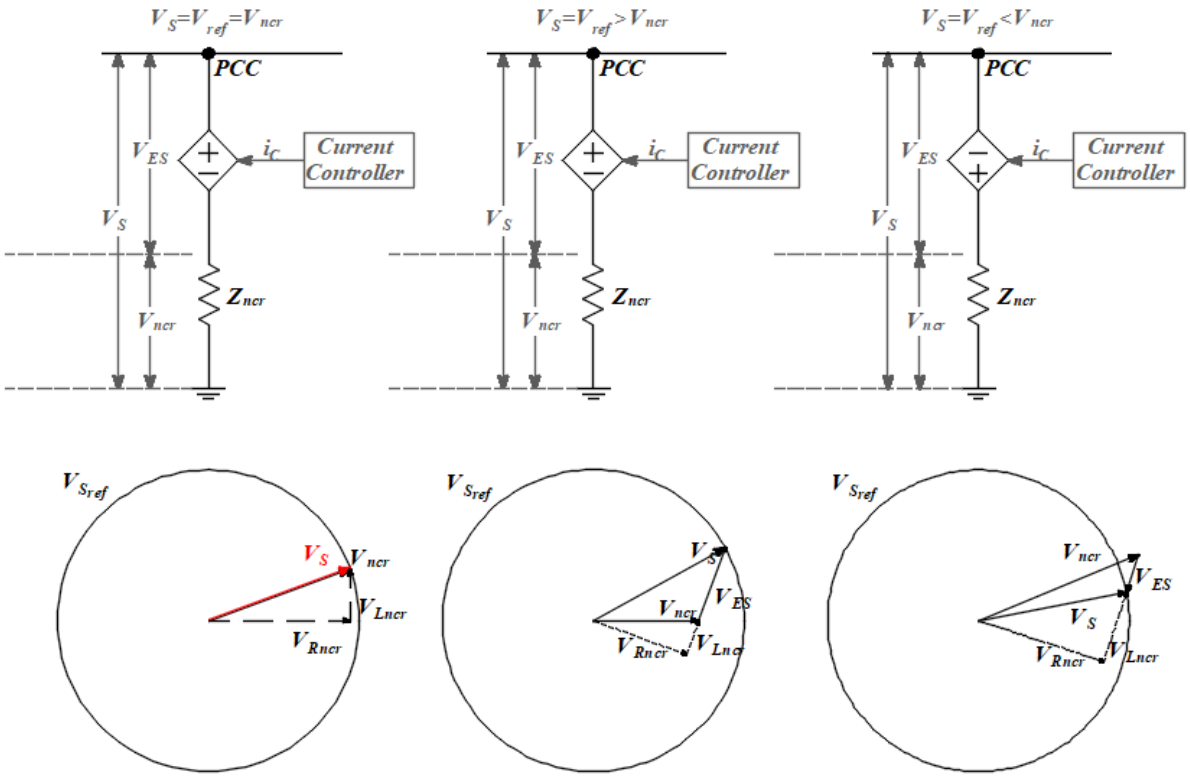

Figure 2. The operation modes and phasor voltage diagram

2.3. Controlling method of electric spring

In this study, the control of ES has been designed as combining two separate control loops in a way to provide voltage regulation and eliminate voltage harmonics, simultaneously. Each control loop has been indicated separately on the control block diagram within rectangular frames as shown in Figure 3.

In the voltage regulation control loop, the RMS value of the fundamental component of PCC voltage (V_{s1}) is compared with a reference value and the error is sent to the PI controller. In order to obtain the amplitude of the modulation index whose value is between 0 and 1, the PI output is multiplied by a proper gain (k) and its absolute value is taken. Whether the rms value of the V_S voltage is smaller or greater than the reference voltage value determines the operating region of the ES. PLL block has been used to determine the phase angle of non-critical load current. In order to ensure that the controlled voltage V_{ES} and noncritical load current are perpendicular to each other, 90 degrees is added or subtracted from the angle value obtained from the PLL block according to the output sign of the PI block. If the value at the output of the PI controller is negative, 90 degrees is added to the phase angle of the current and the ES is operated in inductive mode. However, ES is operated in capacitive mode in case of the value at the PI output is positive. In order to obtain the voltage control signal, the amplitude value from the PI output is multiplied by the unit sine waveform whose phase angle is determined according to the operating region of the ES.

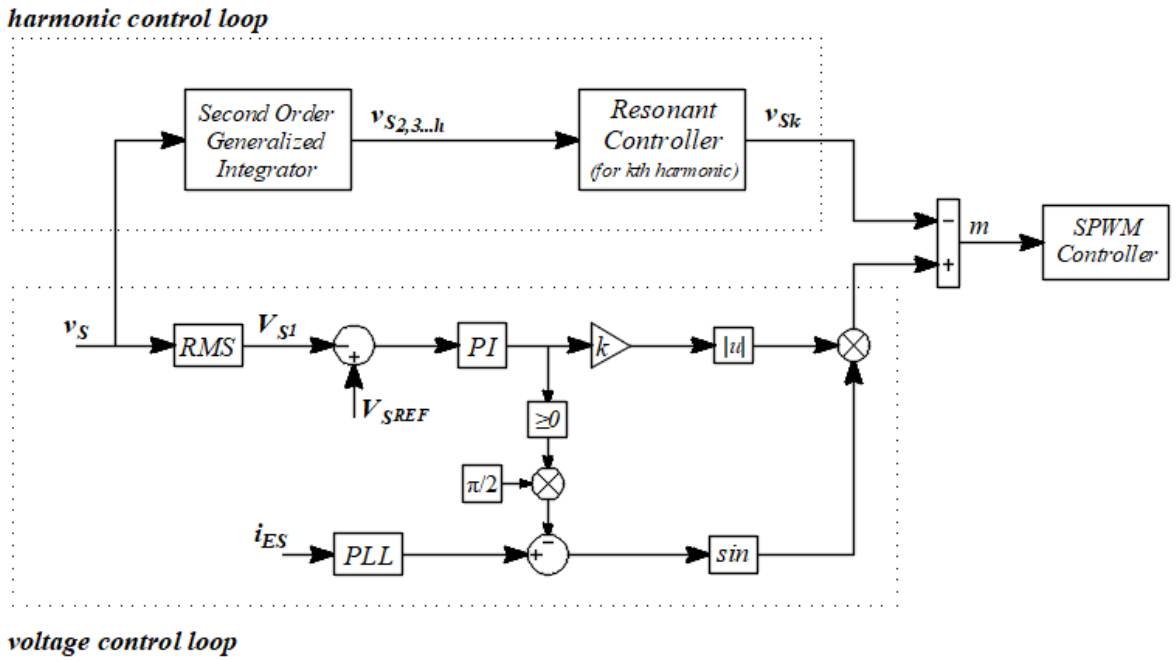

Figure 3. Control block diagrams of electric spring

The harmonic control loop proposed by Kanjiya & Khadkikar (2013) is used to reduce PCC voltage harmonics. Harmonic control loop has been implemented in two steps. In the first step, the harmonic content of the distorted PCC voltage is extracted by using Second Order Generalized integrator (SOGI) structure. The transfer function of SOGI is given in (3). In the second step, multiple resonant controller (MRI) structure has been used to determine the harmonic order to be eliminated. The transfer function of the resonant controller is given in (4).

$$TF_h = \frac{v_{sh}(s)}{v_s(s)} = \frac{s^2+w^2}{s^2+kws+w^2} \quad (3)$$

$$TF_r = \sum_n \frac{2k_n w_c s}{s^2+2w_c s+w_n^2} \quad (4)$$

In (3), w is the angular frequency, k is the damping factor. In Equation-4, w_c is the controller band-width, k_n is the resonant gain, and w_n is the n^{th} harmonic angular frequency to which controller is tuned for.
The damping factor in SOGI and the resonant gain in MRI has been determined by considering the signal from voltage control loop. In order to have control signals in the defined range, damping factor and resonant gain have been chosen as 10 and 0.005 respectively. Thus, the signals from the harmonic control loop have been scaled to the magnitudes that the signal from the voltage control loop can carry.

3. Simulation results

A test system has been modelled in MATLAB/Simulink® by using SimPower blocks to verify the voltage regulation and harmonic elimination performances of the electric springs with different power inverter topologies, namely HFB-ES, FB-ES and NPC-ES. The schematic diagram of the simulated test system is illustrated in Figure 4.

V_{AC} represents the equivalent power supply for a weak point in the network. It is arranged to have a waveform containing the fundamental component and the 5th harmonic to verify the harmonic elimination performance of the ES. In order to test the voltage regulation performance of the ES at different voltage levels, V_{AC} has been varied in three different cases as nominal, voltage sag and over voltage. Simulated test system parameters are given in Appendix.

When the simulation results for the voltage regulation are examined, the performances of three different ES formed with half bridge, full bridge and NPC-MLI topologies are quite close to each other such that all ES's have provided the reference voltage value (220V RMS) on the PCC at the same time. Therefore, for the simplicity, only the HB ES simulation results are shown in Figure 5. In the simulation carried out, the PCC voltage has been arranged as nominal voltage in the range of 0-3 s, undervoltage in the range of 3-8 s, and overvoltage in the range of 8-15 s.

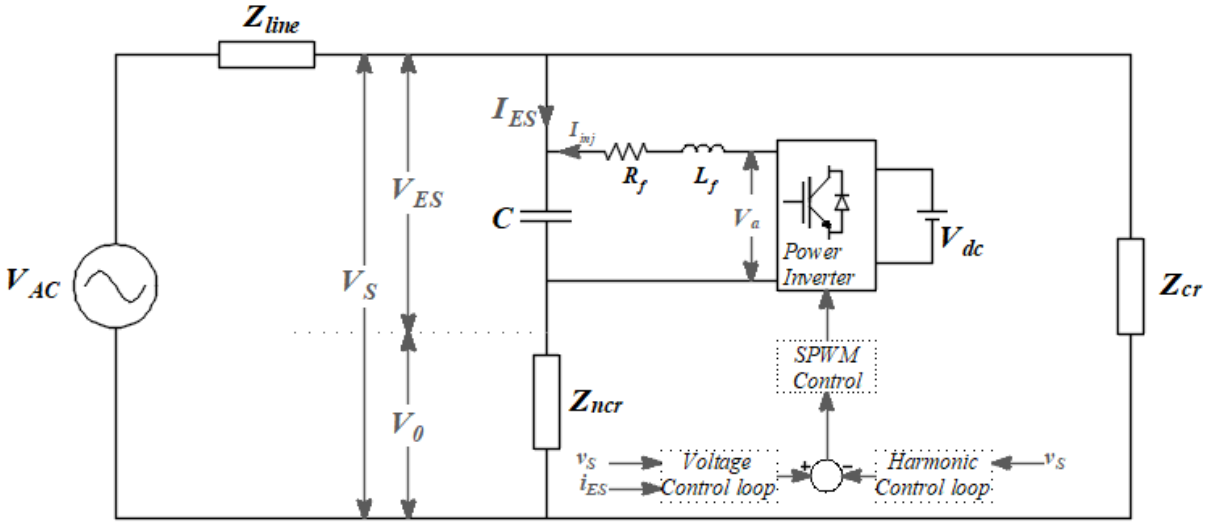

Figure 4. Power system model used in simulations

When the simulation results were examined, it has been seen that ESs with different inverter topologies have reacted to the voltage change on each interval and succeeded to regulate the voltage at the PCC point to the desired reference value, with a very close performance. However, these ESs are expected to differ in terms of their disruptive effects on the system or their success in harmonic elimination, since they have different numbers of semiconductor switching elements within their structure.

In order to figure out the disruptive effect of ES on the system, two different simulations have been performed, with and without the ES. For the case without ES, the capacitor in the same branch as the non-critical load has been removed, leaving only critical and non-critical loads on the load side of the system model. In this case, the input voltage has been adjusted as 220V RMS at the PCC and it has been distorted by including fifth harmonic component. The THD value at PCC has been observed to be 4.44% for this case. In the case that includes ES, the voltage at the PCC point has boosted by the capacitor which is connected to output of ES. The ES have operated within the system as compensating the voltage-boosting effect of the capacitor. Under these conditions, ES has again achieved to regulate the PCC voltage to the desired value, but the THD value has increased to 5.23%.

As can be seen from the results obtained, the activities of the ES in the system create a disruptive effect on the system. The control of the ES can be improved as to eliminate harmonics in the PCC voltage. Thus, ES can exhibit an additional function as harmonic filter besides voltage regulation. For this purpose, by adopting the control approach suggested in the literature (Figure 3), a harmonic control loop has been included in parallel with the voltage control loop. A case study has been conducted to observe the changes on the voltage waveforms and modulation index as a result of the activity of the harmonic control loop. At first, the harmonic control loop was deactivated, and it has been activated in the control loop after two second and the system has been operated for a while. While the THD of the voltage at the PCC point was 6.78%, this value decreased to 4.26% with the activation of the ES and harmonic control loop. This effect can be seen obviously from the improvement on the voltage waveform of the critical load, given in Figure 6.

ESs formed with different inverter topologies (HB, FB, and NPC-MLI) are simulated by applying the above-mentioned input voltages with the control approach shown in Figure 3. The results obtained from the simulations (Table 1) have been examined in terms of voltage regulation and harmonic elimination capabilities.When Table 1 is examined, all ESs provided the desired voltage value in PCC. Among the considered ES types, NPC-ES shows the best performance in terms of harmonic elimination.

As can be seen from the Table – 1, the lowest values for the voltage and current THD and TDD (Total Demand Distortion) on the critical load has been obtained in the case with NPC-ES, for all intervals. The second-best performance in terms of harmonic elimination has been achieved by FB-ES. When the THD values of the voltage and current waveforms of the critical load obtained for all cases are compared, the harmonic elimination performances of HB-ES and FB-ES are close to each other, but NPC-ES outperforms these two ES types by far. In systems with multiple loads connected from a single point, the TDD value is more appropriate to express the amount of distortion in the current. The TDD values calculated over the simulation results also support the findings above.

In order to eliminate the harmonics in the input voltage, the ES injects a current containing inverse harmonics into the system. This non-sinusoidal current creates a non-sinusoidal voltage across the capacitor (Ves) in series with the non-critical load. Thus, the non-critical load voltage distorts by the effect of the voltage across the capacitor. The level of distortion is directly proportional to the success of the ES in eliminating harmonics. A current with a more distorted waveform is required for more successful harmonic elimination. When the THD values of non-critical load voltages are examined from the table, it has been seen that the highest deterioration occurs with NPC-MLI ES.

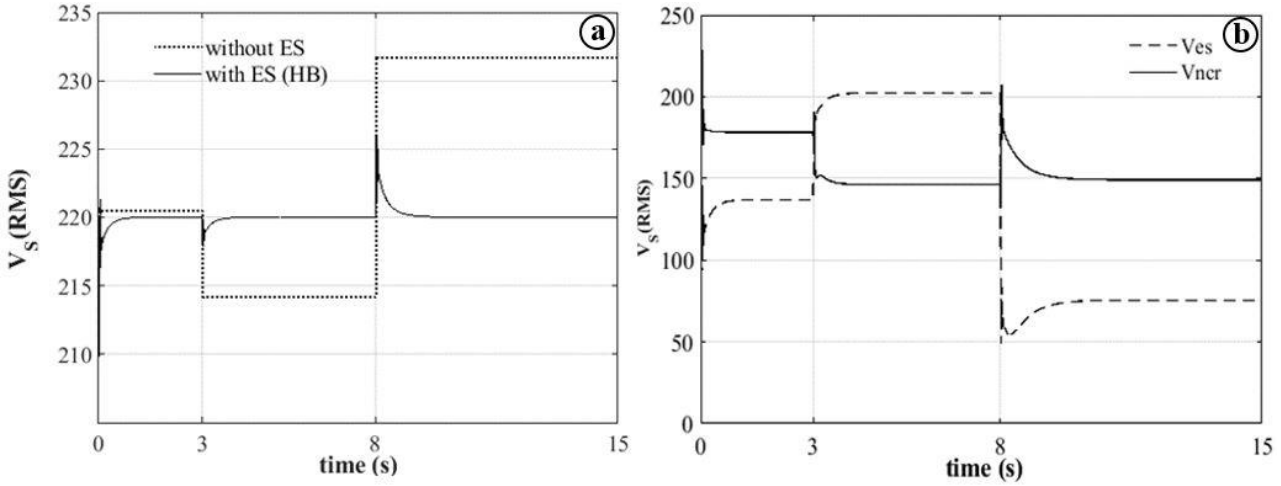

Figure 5. (a) PCC voltage RMS variation with and without ES (b) variations of ES voltage RMS and noncritical load voltage RMS

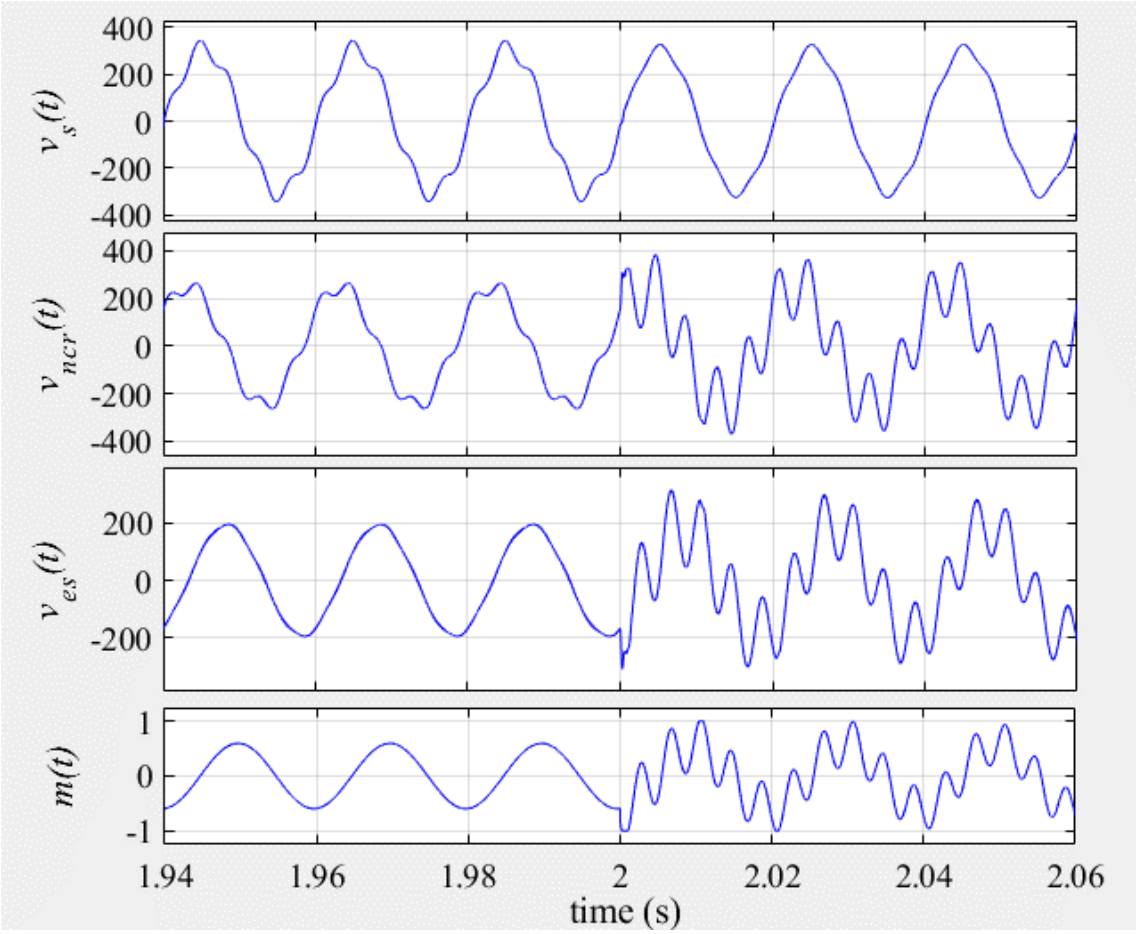

Figure 6. Voltage waveforms and modulation index change after harmonic control loop activation

Table 1. Simulation results at time intervals of 0-3 seconds, 3-8 seconds and 8-15 seconds

			Voltage (V_1)	**Current (I_1)**	**THD_V (%)**	**THD_I (%)**	**TDD (IL=30A)**
Time interval 0-3 s V_1=314 V(peak) V_5=20 V (peak)	Half Bridge ES	Critical Load	220.23	4.69	4.58	2.07	0.32
		Noncritical Load	178.99	18.64	10.04	4.23	2.62
	Full Bridge ES	Critical Load	220.16	4.69	4.26	1.92	0.32
		Noncritical Load	179.24	18.61	11.98	5.05	3.13
	NPC ES	Critical Load	220.09	4.69	3.07	1.38	0.22
		Noncritical Load	179.95	18.51	19.28	8.12	4.99
Time interval 3-8 s V_1=305 V(peak) V_5=20 V (peak)	Half Bridge ES	Critical Load	220.33	4.70	4.69	2.12	0.33
		Noncritical Load	146.99	15.28	11.40	4.80	2.44
	Full Bridge ES	Critical Load	220.34	4.69	4.33	1.96	0.31
		Noncritical Load	148.00	15.34	14.00	5.90	3.01
	NPC ES	Critical Load	220.22	4.70	3.32	1.51	0.24
		Noncritical Load	147.91	15.17	21.82	9.18	4.62
Time interval 8-15 s V_1=330 V(peak) V_5=20 V (peak)	Half Bridge ES	Critical Load	220.22	4.69	4.55	2.06	0.32
		Noncritical Load	150.22	15.59	12.21	5.15	2.67
	Full Bridge ES	Critical Load	220.31	4.70	4.37	1.98	0.31
		Noncritical Load	152.30	15.79	13.32	5.61	2.95
	NPC ES	Critical Load	220.17	4.69	3.19	1.44	0.22
		Noncritical Load	150.38	15.40	22.32	9.40	4.80

3. Conclusions

In this study, the voltage regulation and harmonic elimination performances of three different ESs consisting of HB, FB and NPC-MLI are compared. Considering the simulation results, it has been observed that three types of ES give similar results in terms of voltage regulation. However, they differ in terms of their success in harmonic elimination. When the simulation results are compared, the THD values for the voltage and current of the critical load are ordered from lowest to highest as NPC MLI ES, FB ES, and HB ES. Another superiority of using NPC-MLI in ES is requiring a lower DC voltage at the input, so the semiconductor switching elements are exposed to lower dv/dt. On the other hand, NPC-MLI ES has a drawback as including more semiconductor switching devices than the alternatives, HB-ES and FB-ES. Therefore, controlling inverter is more complicated and the overall system cost is higher than the HB and FB.

The desired voltage level at the critical load can be obtained and the distortion can be reduced in all cases as obtained from simulation results. However, the situation is different for the non-critical load. As a result of the improvements provided in the critical load voltage, it can be seen that the distortion of non-critical load voltage has increased. Harmonics in the current and the voltage waveforms cause losses. By reducing the THD value at the critical load voltage, power losses over the critical load are prevented. On the other hand, the losses on the non-critical load are increased since the distortions in the voltage and the current waveforms are high. The simulation results obtained, and findings remarked in the study may guide to the practitioners to decide on the inverter types which is most convenient for their applications.

As a future work, real-time hardware implementation of the system is planned to be build. In addition, examining the cumulative effects that will occur in a system with more than one smart load may take place in future studies.

Author contribution

In this study, all authors jointly simulated the system, wrote the manuscript and interpreted the results.

Declaration of ethical code

The authors of this article declare that the materials and methods used in this study do not require ethical committee approval and/or legal-specific permission.

Conflicts of interest

The authors declare that there is no conflict of interest.

References

Chaudhuri, N. R., Lee, C. K., Chaudhuri, B., & Hui, S. Y. R. (2014). Dynamic modeling of electric springs. *IEEE Transactions on Smart Grid*, *5*(5), 2450–2458. https://doi.org/10.1109/TSG.2014.2319858

Daratha, N., Das, B., & Sharma, J. (2014). Coordination between OLTC and SVC for voltage regulation in unbalanced distribution system distributed generation. *IEEE Transactions on Power Systems*, *29*(1), 289–299. https://doi.org/10.1109/TPWRS.2013.2280022

Duman, T. (2021). Single phase 5-level NPC multilevel inverter using level-shifted sinusoidal PWM. *International Conference on Advances in Engineering, Architecture, Science and Technology (ICA-EAST 2021)*, (pp. 130–137), Erzurum

Gajbhiye, K., Dahiwale, P., Bharti, S., Pawar, R., Gawande, S. P., & Kadwane, S. G. (2018). Five-level NPC/H-bridge MLI based electric spring for harmonic reduction and voltage regulation. *2017 International Conference on Smart Grids, Power and Advanced Control Engineering (ICSPACE)* (ss. 203-208), Bengaluru: https://doi.org/10.1109/ICSPACE.2017.8343429

Hui, S. Y., Lee, C. K., & Wu, F. F. (2012). Electric springs - A new smart grid technology. *IEEE Transactions on Smart Grid*. https://doi.org/10.1109/TSG.2012.2200701

Kanjiya, P., & Khadkikar, V. (2013). Enhancing power quality and stability of future smart grid with intermittent

renewable energy sources using electric springs. *Proceedings of 2013 International Conference on Renewable Energy Research and Applications, (ICRERA 2013)* (ss. 918-922), Nagasaki: https://doi.org/10.1109/ICRERA.2013.6749882

Kaymanesh, A., Babaie, M., Chandra, A., & Al-Haddad, K. (2021). PEC inverter for intelligent electric spring applications using ANN-based controller. *IEEE Journal of Emerging and Selected Topics in Industrial Electronics*, *3*(3), 704-714. https://doi.org/10.1109/JESTIE.2021.3095018

Lee, C.-K., Liu, H., Tan, S.-C., Chaudhuri, B., & Hui, S.-Y. R. (2021). Electric spring and smart load: Technology, system-level impact, and opportunities. *IEEE Journal of Emerging and Selected Topics in Power Electronics*, *9*(6), 6524–6544. https://doi.org/10.1109/JESTPE.2020.3004164

Liang, L., Hou, Y., & Hill, D. J. (2020). An interconnected microgrids-based transactive energy system with multiple electric springs. *IEEE Transactions on Smart Grid*, *11*(1), 184–193. https://doi.org/10.1109/TSG.2019.2919758

Muttaqi, K. M., Le, A. D. T., Negnevitsky, M., & Ledwich, G. (2015). A coordinated voltage control approach for coordination of OLTC, voltage regulator, and DG to regulate voltage in a distribution feeder. *IEEE Transactions on Industry Applications*, *51*(2), 1239–1248. https://doi.org/10.1109/TIA.2014.2354738

Palensky, P., & Dietrich, D. (2011). Demand side management: Demand response, intelligent energy systems, and smart loads. *IEEE Transactions on Industrial Informatics*, *7*(3), 381–388. https://doi.org/10.1109/TII.2011.2158841

Pawar, R., Gawande, S. P., Kadwane, S. G., Waghmare, M. A., & Nagpure, R. N. (2017). Five-level diode clamped multilevel inverter (DCMLI) based electric spring for smart grid applications. *Energy Procedia*, 117, 862-869. https://doi.org/10.1016/j.egypro.2017.05.204

Rao, P., Crow, M. L., & Yang, Z. (2000). STATCOM control for power system voltage control applications. *IEEE Transactions on Power Delivery*, *15*(4), 1311–1317. https://doi.org/10.1109/61.891520

Shademan, M., Jalilian, A., & Savaghebi, M. (2021). Improved control method for voltage regulation and harmonic mitigation using electric spring. *Sustainability*, *13*(8), 4523. https://doi.org/10.3390/su13084523

Shuo, Y., Tan, S. C., Lee, C. K., & Hui, S. Y. R. (2014). Electric spring for power quality improvement. *2014 IEEE Applied Power Electronics Conference and Exposition (APEC 2014)* (ss. 2140-2147), Fort Worth, TX: https://doi.org/10.1109/APEC.2014.6803602

Sundar, N. S., Philip, L., Tapasvi, P., Akash, M., & Hiraj, D. (2017). Multilevel inverter based electric spring for voltage regulation and active reactive power control. *1st IEEE International Conference on Power Electronics, Intelligent Control and Energy Systems, (ICPEICES 2016)* (ss. 1-5), Delhi: https://doi.org/10.1109/ICPEICES.2016.7853410

Tapia-Tinoco, G., Garcia-Perez, A., Granados-Lieberman, D., Camarena-Martinez, D., & Valtierra-Rodriguez, M. (2020). Hardware structures, control strategies, and applications of electric springs: A state-of-the art review. *IET Generation, Transmission and Distribution*, *14*(23), 1751-8687. https://doi.org/10.1049/iet-gtd.2019.1813

Wang, M.-H., Yang, T.-B., Tan, S.-C., & Hui, S. Y. (2019). Hybrid electric springs for grid-tied power control and storage reduction in AC microgrids. *IEEE Transactions on Power Electronics*, *34*(4), 3214–3225. https://doi.org/10.1109/TPEL.2018.2854569

Wang, M., He, Y., Xu, X., Dong, Z., & Lei, Y. (2021). A review of AC and DC electric springs. *IEEE Access*, *9*, 14398–14408. https://doi.org/10.1109/ACCESS.2021.3051340

Wang, Q., Cheng, M., Jiang, Y., Zuo, W., & Buja, G. (2018). A simple active and reactive power control for applications of single-phase electric springs. *IEEE Transactions on Industrial Electronics*. https://doi.org/10.1109/TIE.2018.2793201

Wang, Q., Cheng, M., Jiang, Y., Zuo, W., & Buja, G. (2018). A simple active and reactive power control for applications of single-phase electric springs. *IEEE Transactions on Industrial Electronics*, *65*(8), 6291-6300. https://doi.org/10.1109/TIE.2018.2793201

Yan, S., Tan, S.-C., Lee, C.-K., Chaudhuri, B., & Hui, S. Y. R. (2015). Electric springs for reducing power imbalance in three-phase power systems. *IEEE Transactions on Power Electronics*, *30*(7), 3601–3609. https://doi.org/10.1109/TPEL.2014.2350001

Yan, S., Tan, S. C., Lee, C. K., Chaudhuri, B., & Hui, S. Y. R. (2017). Use of smart loads for power quality ımprovement.

IEEE Journal of Emerging and Selected Topics in Power Electronics, 5(1), 504-512. https://doi.org/10.1109/JESTPE.2016.2637398

Yang, T., Liu, T., Chen, J., Yan, S., & Hui, S. Y. R. (2018). Dynamic modular modeling of smart loads associated with electric springs and control. *IEEE Transactions on Power Electronics, 33*(12), 10071–10085. https://doi.org/10.1109/TPEL.2018.2794516

Zheng, Y., Hill, D. J., Song, Y., Zhao, J., & Hui, S. Y. R. (2020). Optimal electric spring allocation for risk-limiting voltage regulation in distribution systems. *IEEE Transactions on Power Systems, 35*(1), 273–283. https://doi.org/10.1109/TPWRS.2019.2933240

Appendix

System Voltages			
Time Intervals	**0-3 s**	**3-8 s**	**8-15 s**
Input voltage ($V_{1_{RMS}}$)	222 V	215 V	234 V
PCC Reference voltage ($V_{ref_{RMS}}$)	220 V		
System Impedance			
	R	***L***	
Line impedance (Z_{line})	0.1315 Ω	3.155 mH	
Noncritical Load	8.6 Ω	13.37 mH	
Critical Load	42.9 Ω	60 mH	
Electric Spring			
Low Pass Filter	R_f	L_f	
	3 Ω	0.5 mH	
Capacitance	13.2 µF		
Inverter Topology	**Half-Bridge**	**Full-Bridge**	**NPC-MLI**
DC voltage	600 V	300 V	300 V
Number of Switches	2	4	8
Switching Frequency	5 kHz	5 kHz	5 kHz